Asian Journal of Mathematics and Computer Research

21(3): 127-144, 2017
ISSN: 2395-4205 (P), ISSN: 2395-4213 (O)

A NUMERICAL STUDY OF TURBULENT NATURAL CONVECTION IN A SQUARE ENCLOSURE USING A TWO EQUATION MODEL

MUTILI PETER MUTISYA[1*] AND AWUOR KENNEDY OTIENO[1]

[1]School of Pure and Applied Sciences, Kenyatta University, Box 43844 – 00100, Nairobi, Kenya.

AUTHORS' CONTRIBUTIONS

This work was carried out in collaboration between both authors. Author AKO gathered the initial data and help to interpret the results. Author MPM designed the study, wrote the algorithm, methodology programming and interpreted the results. Both authors read and approved the final manuscript.

ARTICLE INFORMATION

Editor(s):

(1) Dariusz Jacek Jakóbczak, Technical University of Koszalin, Poland.

Reviewers:

(1) Edisson Sávio de Góes Maciel, Instituto Tecnológico de Aeronáutica, Brazil.
(2) António Félix Flores Rodrigues, University of the Azores, Portugal.
(3) Houari Ameur, University Center of Naâma, Algeria.
(4) Igor Miroshnichenko, Tomsk state university, Russia.
(5) Prasun Dutta, Indian Institute of Engineering Science & Technology, India.

Received: 23rd August 2017
Accepted: 6th October 2017
Published: 4th November 2017

Original Research Article

ABSTRACT

In this study the performance of one numerical turbulence model, $k-\varepsilon$ is accessed. In predicting heat transfer due to natural convection inside an air filled square cavity. Turbulent natural convection in an enclosure plays an important role in the field of heat transfer and buildings environment. Natural turbulent convection is square air cavities having isothermal vertical and highly heat – conducting horizontal walls are compared with the experimental data obtained for these cavities at a varying Rayleigh numbers, 1.8 x 10^9, 1.44 x 10^{10} and 1.15 x 10^{11}. In carrying out numerical investigations, a two – dimensional, low turbulence, two – parameter $k-\varepsilon$ model known as the Low – Reynolds – number $k-\varepsilon$ turbulence model was used. The vorticity – vector potential formulation was used to eliminate the need to solve the pressure terms. The vorticity, vector potential energy and two – equation model with their boundary conditions were solved using finite difference approximations. The results of the investigation are presented for the distribution of the velocity and temperature components. The non – linear terms $\overline{u_i u_j}$ and $\overline{u_i \theta}$ in the averaged momentum and energy equations respectively are modelled using the $k-\varepsilon$ model to close the governing equations. The cavity is maintained at 313K on the hot wall and 293K on the opposite cold wall. The horizontal walls are adiabatic. The results obtained show that as the Rayleigh number increases, the values of the stream function increases. As the Rayleigh number increases, uniform distribution of heat inside the cavity is achieved.

Keywords: Turbulent natural convection; heat transfer; square enclosure; Rayleigh number.

**Corresponding author: Email: petermutili@gmail.com;*

NOMENCLATURES

Br	*Brinkman Number,* = $\mu u^2/k\Delta T$
C_p	*Specific Heat Capacity,* J/kgK
Gr	*Grashof Number,* = $\beta g\Delta TL^3\,\rho^2/\mu^2$
g	*Gravitational Acceleration,* m/s^2
H	*Heat Transfer Rate, W*
h	*Heat Transfer Coefficient,* W/m^2K
I	*Radiation Heat Transfer Intensity,* W/m^2
λ	*Thermal Conductivity of the Fluid,* W/mK
L	*Enclosure Wall Length,* m
Nu_c	*Convection Nusselt Number,* = $Q_{conv}/Q_{cond} = hH/K$
Nu_r	*Radiation Equivalent Nusselt Number,* = Q_{rad}/Q_{cond}
Nu_t	*Total Nusselt Number,* = $(Q_{conv} + Q_{rad})/Q_{cond}$
P_r	*Prandtl Number,* = $(\mu C_p)/K$
Q_{conv}	*Convection Heat Transfer, W*
Ra	*Rayleigh Number,* = $g\beta\Delta TL^3/v\alpha$
RC_n	*The New Dimensionless Group,* = $Nu_c/Nu_r = Q_{conv}/Q_{rad} \approx h/\sigma f_{(L,\varepsilon)}T^3$
Sh	*Any other Heat Sources,* W/m^3
T	*Temperature, K*
T_r	*Temperature Ratio,* = T_h/T_c
U_τ	*Shear Velocity* $\left(=\sqrt{(\tau/\rho)}\right)$, m/s
x, y	*Horizontal and Vertical Coordinates,* m
y^+	*Dimensionless Distance,* = $\rho U_\tau y/\mu$

GREEK SYMBOLS

α	*Thermal Diffusivity,* m^2/s
β	*Thermal Expansion Coefficient,* $\alpha\, 1/K$
ΔT	*Temperature Difference between Hot and Cold Walls, K*
V	*Kinematic Viscosity,* m^2/s
μ	*Dynamic Viscosity,* Ns/m^2
σ	*Stefan – Boltzman Constant* $(= 5.672\,X10^{-9}), W/(m^2K^4)$
τ_w	*Local Wall Shear Stress,* N/m^2
ρ	*Density,* kg/m^3
Ω	*Hemispherical Solid Angle,* rad
θ	*Dimensionless Temperature* = $(T - T_c)/(T_H - T_c)$
ψ	*Stream Function* (m^2/s)
ψ_{dim}	*Dimensionless Stream Function*
V_t	*Turbulent Kinematic Viscosity,* m^2/s
$\delta_{i,j}$	*Kronecker Delta*
ε	*Dissipation Rate per Unit of Turbulent Kinetic Energy* s^{-1}
ϕ	*Dissipation Function*
Δt	*Time Interval*
∂	*Differential Operator*
∇	*Del Gradient Operator* $i\frac{\partial}{\partial x} + j\frac{\partial}{\partial y}$
∇^2	*Laplacian Operator* $\frac{\partial^2}{\partial x^2} + \frac{\partial^2}{\partial y^2}$
ξ	*Non – Dimensional Temperature Difference*
δ	*Central Difference Operator*
ϕ'	*Fluctuating part of* ϕ

SUBSCRIPTS AND SUPERSCRIPTS

c	*Cold Wall*
h	*Hot Wall*
t	*Turbulent*
–	*Mean Value*

1 Introduction

Most flows occurring in nature and engineering applications are turbulent. The boundary layer in the earth's atmosphere is turbulent, jet streams in the upper troposphere are turbulent and cumulus clouds are in turbulent motion. The water currents below the surface of the oceans are turbulent. The Gulf Stream is a turbulent wall – jet kind of flow. The photospheres of the sun and photospheres of similar stars are in turbulent motion; inter – stellar gas clouds are turbulent, the wake of the earth in the solar wind is presumably a turbulent wake. Boundary layers growing on aircraft wings are turbulent.

The study of turbulence clearly is an interdisciplinary activity which has a very wide range of applications. In fluid dynamics laminar flow is the exception, not the rule, one must have small dimensions and high viscosities to encounter laminar flow. Most of the dynamics of turbulence is the same in all fluids, whether they are liquids or gases. If the Reynolds number of the turbulence is large enough the major characteristics of turbulence flows are not controlled by molecular properties of fluid in which the turbulence occurs.

Since the equations of motion are non – linear, each individual flow pattern has certain unique characteristics that are associated with its initial and boundary conditions. No general solution to the Navier – Stokes equation is known, consequently, no general solutions to problems in turbulent flows have many characteristics in common. We disregard the uniqueness of any particular turbulent flow and concentrate on the discovery and formulation of laws that describe entire classes or families of turbulent flows.

The Reynolds number of a flow gives a measure of the relative importance of inertia forces and viscous forces. In experiments on fluid systems it is observed that at values below the so called critical Reynolds number Re_{cri}, the flow is smooth and adjacent layers of fluid slide past each other in an orderly fashion. If the applied boundary conditions do not change with time the flow is steady. This regime is called laminar regime. At values of the Reynolds number above Re_{cri}, a complicated series of events takes place which eventually leads to a radical change of the flow character, in the final state the flow behaviour is random and chaotic. The motion becomes intrinsically unsteady even with constant imposed boundary conditions. In this study turbulent natural convection in a square enclosure is considered.

The vertical walls are isothermal while the horizontal walls are adiabatic. The hot walls are kept at 313K and the other cold wall at 293K creating a temperature difference of 20K. The fluid in consideration is air having a Prandtl number 0.71. The aspect ratio is kept constant (Ar=1). The length variations of the enclosure varied the Rayleigh numbers from 1.80×10^{9},1.44×10^{10} and 1.15×10^{11} respectively. The operating temperature inside the enclosure of the air is 303K. The $k - \varepsilon$ model has an extensive and long documented history of use, in this study the standard $k - \varepsilon$ model was used.

2 Literature Review

Turbulent natural convection in enclosures is receiving increasing research attention due to its wide application such as multi – layered walls, multi-pane windows, and electric component cooling, energy transfer in a room and buildings and other enclosed spaces. A significant number of experimental and numerical works have been carried out in the past in an attempt to understand turbulent flow in enclosures. The initial study was made by [1].

[2] studied a two-dimensional $k-\varepsilon$ model in a cubical enclosure heated from below, cooled on the portion of one vertical and insulated on the other.

[3] did an analytical and numerical study on steady natural convection in square enclosures heated from below and cooled along one side. The study indicated that the boundary condition of heating from below is quite different from the case of cooling from below and heating on one vertical wall. Asymptotic expressions were found for the temperature and heat transfer rates near the flux singularity on the enclosure floor.

[4] carried out a numerical study for two dimensional enclosed cavity with boundary conditions which simulate a heated room. The study showed that heat transfer depended on temperature difference.

[5] investigated turbulence flow in a three-dimensional enclosure containing a convectional heater built into one wall and having a window in the same wall. The size of the window was varied but the centre was fixed with respect to the heater. The result indicated that the rate of heat transfer is higher for a larger window than for a small window as the Rayleigh number increases.

[6] investigated natural convection in rectangular enclosures heated from below and symmetrically cooled from the sides using the stream function – vorticity formulation for Rayleigh numbers ranging from 10^3 to 10^7 and aspect ratio varying from 1 to 9. The influences of Rayleigh number (Ra), Prandtl number (Pr) and aspect ratio on the motion and on the energy transport were reported. Numerical values of Nusselt numbers as a function of Ra were also reported with little influence of Pr.

[7] carried out a computational study of turbulent natural convection in a side-heated near cubic enclosure at a Rayleigh of 4.9 $\times 10^{10}$ using Reynolds-averaged Navier – Stokes equations (RANS) approaches. Their computations were performed with both two-dimensional and three dimensional codes using low – Reynolds number $k-\varepsilon$ model of Chien and advanced second moment closure is better in capturing thermal three-dimensional effects and strong streamlines curvature at the corners.

[8] a two–dimensional direct numerical simulation of the natural convection flow of air in a differentially heated square was performed for Rayleigh number of 10^{10}, the results showed that the average Nusselt number is a function of the aspect ratio at constant Ra.

[9] investigated turbulent convection in a rectangular enclosure having finite thickness heat conducting walls at local heating at the bottom of the cavity. Detailed results including streamlines, temperature profiles and correlation for the average Nusselt number of Grashof number have been obtained.

[10] investigated the results of simulation of natural turbulent convection in a square air cavity measuring 0.75 m x 0.75 m and having isothermal vertical and highly heat conducting horizontal walls are compared with the experimental data obtained for this cavity at a Rayleigh number equal to 1.58 x 10^9. In carrying out numerical investigations, a two dimensional low -turbulence, two parameter $k-\varepsilon$ turbulence model was used. The model was also used in calculating forced turbulent convection in a low velocity channel with a backward facing step. The results of modelling are compared with experimental data on heat transfer in a turbulent separation flow downstream of the step. In both cases a satisfactory agreement of the measured values with those predicted by the $k-\varepsilon$ turbulence model is obtained.

[11] investigated Rayleigh number effect on the turbulent heat transfer within a parallelepiped cavity. The purpose was about 3-D study of natural convection within cavities. The turbulent natural convection of air in an enclosed tall cavity with high aspect ratio (Ar = H/W = 28.6) is examined numerically. $k-\varepsilon$ model and k-ω model provided an excellent agreement with experimental data. In order to choose the best model the averaged Nusselt number is compared to the experiment and other numerical results. A 3-D numerical study

has been investigated using two one-point closure turbulence models. The RNG model was developed using Re-Normalisation Group (RNG) methods to renormalise the Navier – Stokes equations, to account for the effects of smaller scales of motion and the SST $k-\omega$ turbulence model is a two – equation eddy – viscosity model which the numerical results are compared to the experimental data made by [12] for the air turbulent natural convection.

[13] numerically investigated a steady buoyancy – driven flow of air in a partially open square 2-D cavity with internal heat source, adiabatic bottom and top walls and vertical walls maintained at different constant temperatures. The influence of the temperature gradient between the vertical walls was analysed for $Ra_e = 10^3 - 10^5$ while the influence of the heat source was evaluated through the relation $R = Ra_i / Ra_e$, investigated at between 400 and 2000. For a low Rayleigh number it is found that the isotherm plots are smooth and follow a parabolic shape indicating the dominance of the heat source. The numerical results show a significant influence of the opening on the heat transfer in the cavity. The study investigated the variation in the streamlines and isotherms of a square cavity as a function of different values of internal and external Rayleigh numbers.

[14] investigated attic design and construction have significant impacts on residential buildings energy performance. In order to understand how passive ventilation rates affect ridge-vent attic's performance a two dimensional steady state finite volume model is employed to simulate the buoyancy driven turbulent ventilation and heat transfer in a triangular attic space of a gable-roof residential building under winter conditions.

The v2f model is used to analyse the turbulent air flow and natural convection heat transfer inside the attic. The simulation results reveal that symmetrical air flow patterns exist in a vented attic in contrast to the asymmetrical air flow patterns found in a sealed attic [14].

They concluded that for all the investigated cases air flow in vented attics tends to be symmetric in contrast to the asymmetric pattern found for air flow in sealed attic.

[15] reviewed recent developments of turbulence models for natural convection enclosures. The turbulence models considered in the present study are the two-layer $k-\varepsilon$ model, the shear stress transport (SST) model, the elliptic – relaxation (v2-f) model and the elliptic-blending second-moment closure (EBM) the mathematical formulation of the above turbulence models and their solution method are presented. The relative performance of turbulence models are examined and their successes and shortcomings are addressed.

[16] investigating the effects of natural convection with and without the interaction of surface radiation in square and rectangular enclosures have been studied numerically and theoretically. The analysis were carried out over a wide range of enclosure aspect ratios ranging from 0.0625 to 16, including square enclosures in sizes from 40cm to 240cm, with cold wall temperatures ratios ranging from 283 to 373K and hot to cold temperature ratios ranging from 1.02 to 2.61. Turbulence was modelled using the RNG $k-\varepsilon$ model with a non-uniform grid. The Discrete Transfer Radiation Model (DTRM) was used for radiation simulation. The problem of turbulent natural convection with the interaction of surface thermal radiation in square and rectangular enclosures have been analysed with different fluids, enclosures sizes, aspect ratios and cold and hot wall temperatures. The problem was solved using variable fluid properties.

[17] investigated turbulent double-diffusive natural convection in a square cavity. Only several $k-\varepsilon$ models were developed to investigate turbulent double-diffusive convention and there is no attempt to use Large Eddy Simulation (LES). They proposed a novel LES-based lattice Boltzmann (LB) Model to simulate such turbulent convectional flow.

[18] investigated laminar and turbulent natural convection inside concentric spherical shells with isothermal cold and hot boundaries was numerically investigated up to Rayleigh number values $Ra \leq 10^{12}$ and $Pr = 0.71$. The study utilizes Direct Numerical Simulation (DNS). Large Eddy Simulation (LES) and Reynolds Averaged Navier-Stokes (RANS) approaches for investigation of the laminar transitional and fully

developed turbulent flow regimes respectively. It was found that the steady state flow pattern is axisymmetric and characterized by a single Convection Cell.

[19] performed a numerical study of a turbulent natural convection problem with a compressible Large – Eddy Simulation. In a natural convection the fluid is accelerated by local density differences and a resulting pressure gradient. Density changes due to temperature differences are considered in the numerical model by a compressible coupled model. The fluid properties profiles e.g. temperature and velocity show an asymmetrical which is caused by the non – Boussinesq effects of the fluid. A non - Boussinesq, compressible LES was performed for a turbulent natural convection in an air - filled enclosed container with vertical height walls. In the experiment the set up consisted of conducting later walls, while in the numerical simulation two different related boundary conditions were tested.

[20] investigated the natural convection induced by temperature difference between a cold outer square enclosure and two hot inner circular cylinders. A two dimensional solution for natural convection in an enclosure with inner cylinders is obtained using an accurate and efficient immersed boundary method. The result in the case of the two cylinders are compared with those in the case of the single cylinder. The distribution of the isotherms and streamlines eventually reaches a steady state or changes his state from steady to unsteady.

[21] presented a study on free convection in a porous square cavity saturated with a Newtonian fluid. Computation of laminar and turbulent flow is performed. Discretization of governing equations was obtained with the control volume approach and the system of algebraic equation was relaxed via the simple method. Two energy models were employed namely the one and two temperature models. Results indicated that when the ratio of thermal conductivities equals unity both models give similar results. In conclusion computations for turbulent flow in square cavity fully filled with porous medium were performed.

[22] presented a computational study of turbulent heat transfer through two pass square-duct channel flows with several different turbulence models that were developed to improve near-wall predictions. To evaluate the performance of the advanced wall function (the analytical wall function: AWF) the results were compared with experimental data those by a low Reynolds-number $k - \varepsilon$ model and a convectional wall function (the log-low based wall Function: LWF). The AWF showed the improvements in the heat transfer predictions. In conclusion for the flow field it is confirmed that both the results of the log-low and the AWF models are almost indistinguishable.

[23] numerically studied turbulent natural convection in a rectangular enclosure with varying aspect ratio of 0.5, 1 and 2. The finite volume based solver Fluent with Boussinesq approximations was used to conduct the numerical study. The $k - \omega$ two equation Reynolds Averaged Navier – Stoke Equations – based turbulence model was used for turbulent simulation. The results obtained show that as the aspect ratio increases, the eddies at the top of the hot wall and at the bottom of the cold wall increase and the flow on the two vertical walls tend to exert more force on the stratified core.

3 Methodology

3.1 The governing equations

The general equations governing Newtonian fluid in motion results from invoking the physical laws of conservation of energy, momentum and mass. In turbulent flows the velocity, pressure and temperature at any point in the fluid vary rapidly and randomly with time. In turbulent flows, the conservation laws apply. The equations governing free convections in viscous Newtonian fluid are described using partial differential equations [24] which express the laws of conservation of energy, momentum and mass. These equations are then decomposed by expressing fluid properties as the sum of a mean and a fluctuating value. Moreover, the equations are presented in tensor form and also in Cartesian form useful for computer programming.

$$\frac{\partial \rho}{\partial t} + \frac{\partial}{\partial x_j}(\rho u_j) = 0 \quad (1)$$

$$\rho\left[\frac{\partial u}{\partial t} + u\frac{\partial u}{\partial x} + v\frac{\partial u}{\partial x}\right] = F_x - \frac{\partial p}{\partial x} + \mu\nabla^2 u \quad (2)$$

$$\rho\left[\frac{\partial v}{\partial t} + u\frac{\partial v}{\partial x} + v\frac{\partial v}{\partial y}\right] = F_y - \frac{\partial p}{\partial y} + \mu\nabla^2 v \quad (3)$$

$$\frac{\partial}{\partial t}\rho u_i + \frac{\partial}{\partial x_j}(\rho \mu_i u_j) = -\frac{\partial p}{\partial x_i} + \rho g_i + \frac{\partial}{\partial x_j}\left[\mu\left(\frac{\partial u_i}{\partial x_j} + \frac{\partial u_j}{\partial x_i}\right)\right] + \mu_s \delta_{ij}\frac{\partial u_k}{\partial x_k} \quad (4)$$

$$\frac{\partial}{\partial t}\rho C_p T + \frac{\partial}{\partial x_j}(\rho C_p u_j T) = \frac{\partial}{\partial x_j}\left(\lambda\frac{\partial T}{\partial x_j}\right) + \beta T\left(\frac{\partial p}{\partial t} + \frac{\partial u_j p}{\partial x_j}\right) + \tau_{ij}\frac{\partial u_j}{\partial x_j} \quad (5)$$

3.2 Final set of equations

For simplicity the over-bar indicating time mean values and the fluctuating quantities will be replaced by the upper and lower case letters respectively for the case of velocity components and fluid properties P and T. The final set of equation for turbulent natural convection flows is:

$$\frac{\partial \rho}{\partial t} + \frac{\partial}{\partial x_j}\left(\rho u_j + \overline{\rho u_j}\right) = 0 \quad (6)$$

$$\frac{\partial}{\partial t}(\rho u_i + \overline{\rho u_i}) + \frac{\partial}{\partial x_j}\left(\rho u_i u_j + u_i\overline{\rho u_j}\right) = -\frac{\partial p}{\partial x_j} + \rho g_i + \frac{\partial}{\partial x_j}\left(\tau_{ij} - u_i\overline{\rho u_i} - \rho\overline{u_i u_j} - \overline{\rho u_i u_j}\right) \quad (7)$$

$$\frac{\partial}{\partial t}(c_P\,\rho T + c_P\overline{\rho T}) + \frac{\partial}{\partial x_j}\left(c_p u_j T\right) = \frac{\partial p}{\partial t} + u_j\frac{\partial p}{\partial x_j} + \overline{u_j\frac{\partial p}{\partial x_j}} + \frac{\partial}{\partial x_j}\left(\lambda\frac{\partial T}{\partial x_j} - c_P\overline{\mu t} - c_P u_i t\right) + \phi \quad (8)$$

Where:- $\tau_{ij} = \mu\left(\frac{\partial u_i}{\partial x_j} + \frac{\partial u_j}{\partial x_i}\right) + \mu_s\delta_{ij}\frac{\partial u_k}{\partial x_k}$ (9)

$$\phi = \tau_{ij}\frac{\partial u_i}{\partial x_j} + \overline{\mu\left(\frac{\partial u_i}{\partial x_j} + \frac{\partial u_j}{\partial x_i}\right)\frac{\partial u_j}{\partial x_j}} \quad (10)$$

$$\frac{\partial}{\partial_t}\rho k + \frac{\partial}{\partial x_j}\left(\rho u_j k\right) = \overline{u_j\frac{\partial}{\partial x_j}\mu\left(\frac{\partial u_i}{\partial x_j} + \frac{\partial u_j}{\partial x_i}\right)} - \frac{1}{2}\frac{\partial}{\partial x_j}\overline{\rho u_i u_i u_j} - \rho\overline{u_i u_j}\frac{\partial u_i}{\partial x_j} + \overline{\rho u_i g_i} - \overline{u_j\frac{\partial p}{\partial x_i}} \quad (11)$$

$$\frac{\partial}{\partial t}(\rho\varepsilon) + \frac{\partial}{\partial x_j}\left(\rho u_j\varepsilon\right) = -\frac{\partial}{\partial x_k}\left(\overline{\mu\mu_k\frac{\partial u_i}{\partial x_j}\frac{\partial u_i}{\partial x_j}} + 2v\overline{\frac{\partial u_k}{\partial x_i}\frac{\partial p}{\partial x_i}} - \mu\frac{\partial \varepsilon}{\partial x_k}\right) - 2\mu\left(\overline{\frac{\partial u_i}{\partial x_k}\frac{\partial u_i}{\partial x_j}\frac{\partial u_k}{\partial x_j}}\right) - 2\rho\left(\overline{v\frac{\partial^2 u_i}{\partial x_k \partial x_j}}\right)^2 + 2v\left(\overline{\frac{\partial u_i}{\partial x_j}\frac{\partial \rho}{\partial x_j}g_i}\right) - 2\mu\left(\frac{\partial^2 u_i}{\partial x_i \partial x_k}\right)\mu_k\left(\frac{\partial u_i}{\partial k_j}\right) - 2\mu\frac{\partial u_i}{\partial x_k}\left(\overline{\frac{\partial u_i}{\partial x_j}\frac{\partial u_k}{\partial x_j}} + \overline{\frac{\partial u_j}{\partial x_i}\frac{\partial u_j}{\partial x_k}}\right) \quad (12)$$

3.3 Non-dimensional numbers

Froude number; $Fr = \frac{U_*}{gL_z}$

Reynolds number; $Re = \frac{\rho_z U_* L_z}{\mu_z}$

Eulers number; $Eu = \frac{P_z}{\rho_z U_*^2}$

Pressure number; $Pn = \frac{P_z}{\rho_z C_{Pz} T_z}$

Gravity number; $Gn = \frac{\left(\mu_z g/\rho_z\right)}{C_{Pz} T_z}$

Eckert number; $Ec = \frac{U_c^2}{C_{Pz}\Delta T_*}$

Prandtl number; $Pr = \frac{\mu_z C_{Pz}}{\lambda_z}$

Grashof number; $Gr = \frac{Ra}{Pr}$

Non – dimensional temperature difference; $\zeta = \frac{\Delta T_*}{T_z}$

Rayleigh number; $Ra = \frac{P_z^2 c_{Pz} g \beta \Delta T_* L_z}{\mu_z K_z}$

$$\eta = \beta_z T_z$$

3.4 Mathematical model

A number of heat-transfer problems of structural thermal physics that are connected with calculation of ventilated and unventilated air interlayers in enclosures as well as those of transparent structure's (windows, glass fronts, garret windows etc.) must be solved with allowance for the presence in these constructions of low – turbulence air flows predominantly induced by natural convection. The data on convective heat – transfer coefficients on the surfaces of structures needed for heat – engineering calculations can be obtained from an experiment which however is rather laborious, intensive and of specific nature.

Another route is numerical simulation of air flows and heat transfer. But here, not all models of turbulent flows are suitable for modelling natural convections at small Reynolds numbers. The present investigation was undertaken in order to evaluate the possibility of using one of the variants of the low Reynolds number $k - \varepsilon$ turbulence model for adequate description of heat transfer and flow characteristics at small Reynolds numbers in the above specified range of problems. In what follows for the sake of brevity, this model will be called the $k - \varepsilon$ model.

3.5 Numerical methods

In solving the Governing equations, the finite difference method was used. The partial differential equations are approximated by a set of linear equations relating to the values of the function at each mesh point which results to solutions of algebraic equations. In order to take care of the non – linear character of equations, an iteration procedure is used. The process of replacing the partial differential equation with an algebraic finite – difference is called finite – difference discretization or approximation. Finite – difference discretization is done in two levels, discretization of the solution domain and discretization of the governing equations.

3.5.1 Discretization of the solution domain

The turbulent natural convection flow in an enclosure is featured by a thin boundary layer along the walls while the core is thermally stratified. The flow gradients are very large in the boundary layer and require a huge number of grid points. The domain of the solution in this case study, the enclosure is partitioned into a network of uniform square grid with very fine spacing. In the Cartesian coordinate the finite difference grid is comprised of an array of straight lines that run parallel to the $x - y$ axis with spacing Δx and Δy. The accuracy of the numerical computation depends on the size of the grids spacing Δx and Δy.

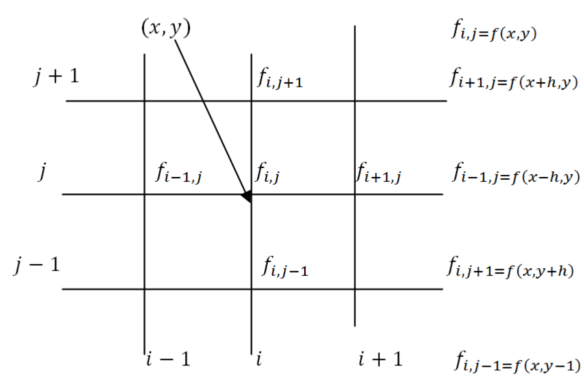

Fig. 1. The location of variables on a structured grid

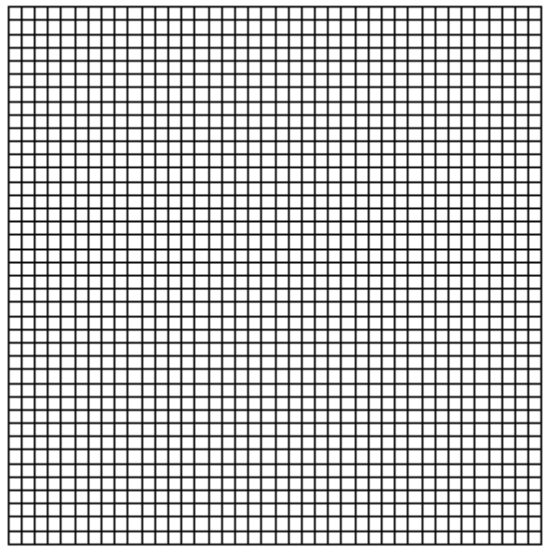

Fig. 2. 40 by 40 computational grids

3.5.2 Discretization of the governing equations

Discretization of the governing equations involves replacing of governing equations with finite difference equation which is then applied sequentially at the internal nodes of the grid to give a system of linear algebraic equations that relate the value of the unknown function *f* at the nodes. The need of replacing the partial differential equation with a finite – difference equation is to generate the values of the function *f* at the nodes (i, j). Expanding using Taylor series expansion of dependent variables *f* about point 0 and 2 as shown in Fig. 3 below:

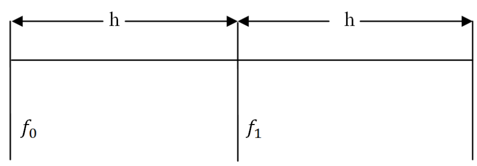

Fig. 3. Three point finite – difference approximation

$$f_0 = f_1 - hf' + \frac{h^2}{2}f'' - \frac{h^3}{6}f''' + O(h^4) \tag{13}$$

$$f_2 = f_1 + hf' + \frac{h^2}{2}f'' - \frac{h^3}{6}f''' + O(h^4) \tag{14}$$

Subtracting equation (1) from equation (2) yields:-

$$f_2 - f_0 = 2hf' + \frac{1}{3}f''' \tag{15}$$

Making $f'$the subject of the formulae:-

$$f' = \frac{f_2 - f_0}{2h} + O(h) \tag{16}$$

Adding equation (1) and equation (2) yields:-

$$f_0 + f_2 = 2f_1 + h^2 f'' + O(h^4) \tag{17}$$

Making $f''$the subject of the formulae:-

$$f'' = \frac{f_0 - 2f_1 + f_2}{h^2} + O(h^4) \tag{18}$$

Where '***h***' is the grid spacing.

Using Taylor series expansion in '***t***' to approximate the time derivative $\frac{\partial f}{\partial t}$ with a first order backward difference method about a grid point (i, j) at the time instant t_{n+1} we have:-

$$\frac{\partial f}{\partial t} = f_{i,j}^{n+1} - f_{i,j}^{n} + O(\Delta t) \tag{19}$$

Using Taylor series expansion to approximate spatial derivatives with second order central difference we have:-

$$\frac{\partial^2 f}{\partial x^2} = \frac{f_{i-1,j}^{n+1} - 2f_{i,j}^{n+1} + f_{i+1,j}^{n+1}}{\Delta x^2} + O(\Delta x^2) \tag{20}$$

and

$$\frac{\partial^2 f}{\partial y^2} = \frac{f_{i,j-1}^{n+1} - 2f_{i,j}^{n+1} + f_{i,j+1}^{n+1}}{\Delta y^2} + O(\Delta y^2) \tag{21}$$

Hence the Laplacian is given by:-

$$\frac{\partial^2 f}{\partial x^2} + \frac{\partial^2 f}{\partial y^2} = \frac{f_{i+1,j}^{n} - 2f_{i,j}^{n} + f_{i-1,j}^{n}}{h^2} + \frac{f_{i,j+1} - 2f_{i,j}^{n} + f_{i,j-1}^{n}}{h^2} = \frac{f_{i+1}^{n} + f_{i-1,j}^{n} + f_{i,j+1}^{n} + f_{i,j-1}^{n} - 4f_{i,j}^{n}}{h^2} \tag{22}$$

This order gives first order accuracy in time and second order accuracy in spatial partial derivatives.

3.6 Mathematical formulation

Fig. 4 shows a schematic diagram of the problem under consideration and the coordinate system. The system to be, considered is a two – dimensional square cavity of width W and height H, where the two vertical are kept at different temperatures, T_h(left wall) and T_c (right wall), $T_h > T_c$. Zero heat flow is assumed at the top and bottom walls (adiabatic). The walls are rigid and no – slip conditions are imposed at the boundaries.

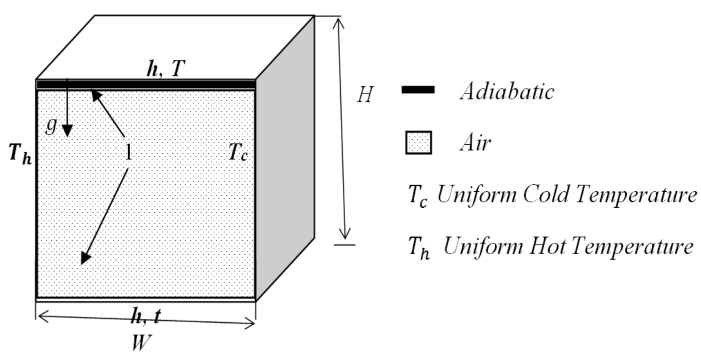

Fig. 4. Geometry and boundary conditions of the model of a cavity: 1 steel sheets of thickness 1.5mm ; H = W = 1.0m,2.0m,4.0m ; T_h = 313K ; T_c= 293K ; T = 303K ; h = $\frac{1W}{(m^2\,^oc)}$

The parameters of the incoming flow (flow velocity or pressure, turbulent kinetic energy k and dissipation of the turbulent kinetic energy, ε are considered known.

Near the wall the following boundary value for k is given;

$$k_{wall} = 0$$

Whereas ε is calculated according to [25] from the formula; $\varepsilon_w = 2v\left(\frac{\partial\sqrt{k}}{\partial n}\right)^2$

In this study the temperature of the hot wall was kept at 313K and the other cold wall at 293K. The aspect ratio$(Ar = H/W = 1)$ was kept constant because the dimensions of the enclosure varied from 1m by 1m, 2m by 2m and 4m by 4m. This variation of length was made in order to vary the values of Rayleigh numbers from 1.80 x 10^9, 1.44 x 10^{10} and 1.15 x 10^{11} respectively. The calculation of the Rayleigh numbers were calculated using the formulae $Ra = \frac{g\beta\rho^2 C_p \Delta T W^3}{\mu K}$. The operating temperature inside the enclosure of the air is 303K.

3.7 Model equations

The model is based on the Low – Reynolds number $k - \varepsilon$ turbulence model with variable coefficients which was described in detail in [26]. The mathematical formulation of the two – dimensional model was made, using the Boussinesq approximation for a viscous incompressible fluid.

It includes the:–

i. Continuity Equation;

$$\frac{\partial U}{\partial x} + \frac{\partial V}{\partial y} = 0 \tag{23}$$

ii. The momentum equations in the X and Y directions (The Navier – Stokes Equations);

$$\frac{\partial U}{\partial t} + U\frac{\partial U}{\partial x} + V\frac{\partial U}{\partial y} = -\frac{1}{\rho}\frac{\partial P}{\partial x} + \frac{\partial}{\partial x}(v + v_t)\left[2\frac{\partial U}{\partial x}\right] + \frac{\partial}{\partial y}(v + v_t)\left[\frac{\partial U}{\partial y} + \frac{\partial V}{\partial x}\right] \tag{24}$$

$$\frac{\partial V}{\partial t} + U\frac{\partial V}{\partial x} + V\frac{\partial V}{\partial y} = -\frac{1}{\rho}\frac{\partial P}{\partial y} + g\beta(T + T_m) + \frac{\partial}{\partial y}(v + v_t)\left[2\frac{\partial V}{\partial y}\right] + \frac{\partial}{\partial x}(v + v_t)\left[\frac{\partial V}{\partial x} + \frac{\partial U}{\partial y}\right] \tag{25}$$

iii. The energy – transfer equation:–

$$\frac{\partial T}{\partial t} + U\frac{\partial T}{\partial x} + V\frac{\partial T}{\partial y} = \frac{\partial}{\partial x}\left[\frac{V}{Pr} + \frac{V_t}{\sigma_t}\right]\frac{\partial T}{\partial x} + \frac{\partial}{\partial y}\left[\frac{V}{Pr} + \frac{V_t}{\sigma_t}\right]\frac{\partial T}{\partial y} \tag{26}$$

iv. The equation of transfer of the kinetic energy of turbulent pulsations:–

$$\frac{\partial k}{\partial t} + U\frac{\partial k}{\partial x} + V\frac{\partial k}{\partial y} = \frac{\partial}{\partial x}\left[v + \frac{V_t}{\sigma_k}\right]\frac{\partial k}{\partial x} + \frac{\partial}{\partial y}\left[v + \frac{V_t}{\sigma_k}\right]\frac{\partial k}{\partial y} + P_k + G_k - \varepsilon \tag{27}$$

v. The equation of transfer of the rate of turbulent – energy dissipation:–

$$\frac{\partial \varepsilon}{\partial t} + U\frac{\partial \varepsilon}{\partial x} + V\frac{\partial \varepsilon}{\partial y} = \frac{\partial}{\partial x}\left[v - \frac{V_t}{\sigma_\varepsilon}\right]\frac{\partial \varepsilon}{\partial x} + \frac{\partial}{\partial y}\left[v + \frac{V_t}{\sigma_\varepsilon}\right]\frac{\partial \varepsilon}{\partial y} + C_1 f_1 \frac{\varepsilon}{k}P_k + C_2 f_2 \frac{\varepsilon^2}{k} + S_\varepsilon \tag{28}$$

vi. The turbulent viscosity v_t is expressed in terms of k and ε from the Prandtl – Kolmogorov relation:–

$$V_t = C_\mu f_\mu \frac{k^2}{\varepsilon} \tag{29}$$

The generation of turbulence P_k in equations (27) and (28) is modelled by the expression:-

$$P_k = V_t\left[2\left(\frac{\partial U}{\partial x}\right)^2 + 2\left(\frac{\partial V}{\partial x}\right)^2 + \left(\frac{\partial U}{\partial y} + \frac{\partial V}{\partial x}\right)^2\right] \tag{30}$$

The source term G_k in equation (17) owing its origin to buoyancy is defined as:–

$$G_k = -g\beta \frac{V_t}{\sigma_t}\frac{\partial T}{\partial y} \tag{31}$$

The complement of the $k-\varepsilon$ model of turbulence with variable coefficient is the source term S_ε in dissipation equation (28) suggested by [27] to correct the turbulence scale near the wall which is defined by the expression:–

$$S_\varepsilon = 0.83\left[\frac{k^{\frac{3}{2}}}{\varepsilon c_1 y} - 1\right]\left[\frac{k^{\frac{3}{2}}}{\varepsilon c_1 y}\right]^2 \frac{\varepsilon^2}{k} \tag{32}$$

Where y is the distance from the wall and $c_1 = \frac{k^{\frac{3}{2}}}{\varepsilon} = 2.5$ in the wall zone of Constant shear stresses of a flow.

3.8 Boundary conditions

3.8.1 Temperature boundary conditions

The non – dimensional was defined by $\theta = \frac{T-T_*}{\Delta T_*}$ where ΔT_* is the characteristic temperature difference between the hot and cold surfaces i.e. $\Delta T_* = T_h - T_c$, the choice of θ ensures that it is bounded and lie between 0 and 1.

The thermal boundary conditions which were used are isothermal and adiabatic conditions. These conditions are represented by the equations:-

$$\left.\begin{array}{l}\theta = constant \\ \frac{\partial\theta}{\partial n} = 0\end{array}\right\} \tag{33}$$

Where *n* refers to the direction normal to a wall. Since the problem involves heating on one wall and cooling on the opposite wall all the remaining four walls of the enclosure are kept adiabatic on the hot and cold walls, the Derichlet boundary conditions are used where $\theta_{hot} = 1 \; and \; \theta_{cold} = 0$.

Neumann boundary condition is used on the remaining four walls i.e. $\frac{\partial\theta}{\partial n} = 0$ for each of four walls.
NB: On the $x-y$ plane;

$$\frac{\partial\theta}{\partial z} = 0$$

3.8.2 Velocity boundary conditions

The conditions in the motion of fluid at a boundary are specified in terms of the velocity. Particles close to a surface do not move along with a flow when adhesive forces are stronger than cohesive forces.
In a closed cavity each boundary is impermeable. Normal component of velocity at each boundary is zero. For example the boundary $x = 0$ in the $y - z$ plane. The velocity component normal to the surface is naturally zero as mass cannot penetrate an impermeable solid surface.

4 Results and Discussion

4.1 Streamlined distribution

A streamline is a path stressed out by a massless particle as it moves with the flow. Velocity is tangent to streamline at every point and mass does not cross streamlines. A streamline is a contour designed to minimize resistance to motion through a fluid. A streamline is an imaginary line in a fluid such that the tangent at any point indicates the direction of the velocity of a particle of the fluid at that point. The result of this study were obtained for the Rayleigh numbers between 1.80×10^8 and 1.15×10^{11}

Fig. 5 shows the distribution of stream function for different Rayleigh numbers with the aspect ratio held constant. In Fig. 5 when $Ra = 1.80 \times 10^9$ there are three circulating vortices which have different sizes. As the Rayleigh number increases the vortices and stream functions increase in number. The streamlines are observed to move up of the left hand side (hot wall) and sink on the right hand side (cold wall) which is consistent with the principle of convection which states that, "warm fluids rise, cold fluids sinks." When the Rayleigh number increases, the buoyancy forces increases leading to increase of the sizes of the re – circulating vortices and the strength of the stream function as shown in Fig. 5(a), (b) and (c).

4.2 Contours of velocity magnitudes

In fluids dynamics, turbulence or turbulent flow is a flow regime characterized by chaotic property changes. These include low momentum diffusion, high momentum convection and rapid variation of pressure and flow velocity in space and time. In turbulent flow, steady vortices appear on many scales and interact with each other. The schematic representation of contours of velocity magnitudes are shown in Fig. 6. As the Rayleigh numbers increase the number of vortices also increase. The streamlines also tend to rise as they appear on the left hand side (hot wall) and sink on the right hand side (cold wall). It is also observed that as the Rayleigh number increase the flow becomes more chaotic showing that the velocity is instantaneously varying as shown in Fig. 6 (a), (b) and (c).

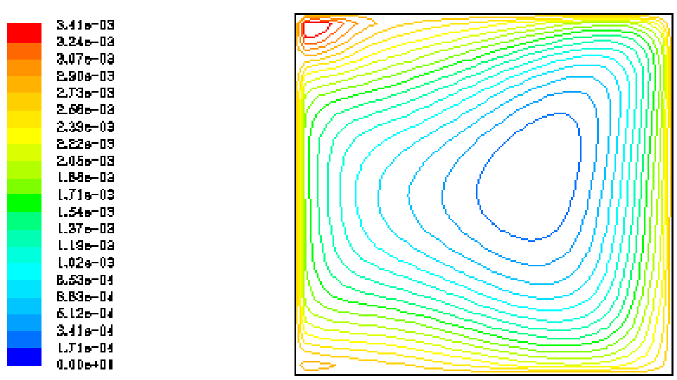

Fig. 5(a). Contours of stream function (kg/s) Ra = 1.80 × 10^9.

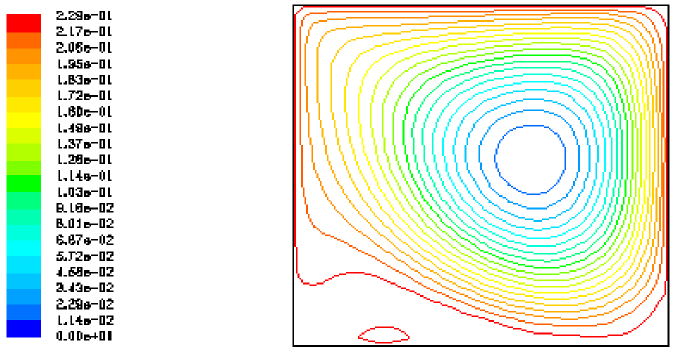

Fig. 5(b). Contours of stream function (kg/s) Ra = 1.44 × 10^{10}

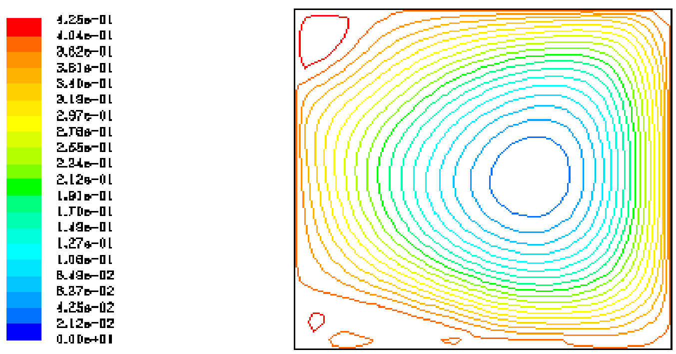

Fig. 5(c). Contours of stream function (kg/s) Ra = 1.15 × 10^{11}.

4.3 Isotherms distribution

An isotherm is a curve on a graph that connects points of equal temperatures. An isotherm should never split, cross or touch another isotherm because then at the crossing point it would have two different temperature values which is physically impossible. Isotherms are created from regularly scheduled, simultaneous temperature readings at different locations. Fig. 7 shows isothermal contours of various Rayleigh numbers. The heat is transferred from the hot wall through the working fluid to the remaining parts of the enclosure. As the Rayleigh number increase the contours of temperature tend to enlarge and rise on the left hand side (hot wall) and sink in the right hand side (cold wall) as shown in Fig. 7(a), (b) and (c). The thickness of the thermal boundary layer is increased with increase of Rayleigh number. As the Rayleigh number increase the contour at the middle tend to decrease towards the left hand side wall (hot wall).

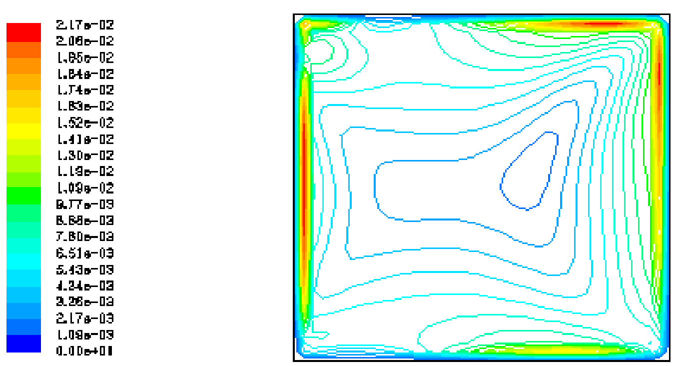

Fig. 6(a). Contours of velocity magnitude (m/s) Ra = 1.80 × 10^9.

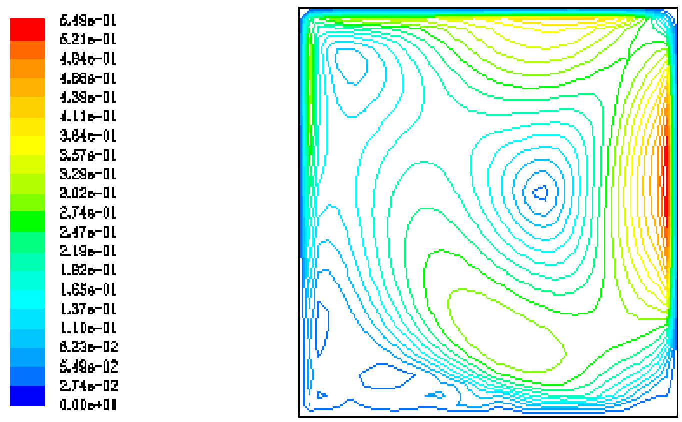

Fig. 6(b). Contours of velocity magnitude (m/s) Ra = 1.44×10^{10}.

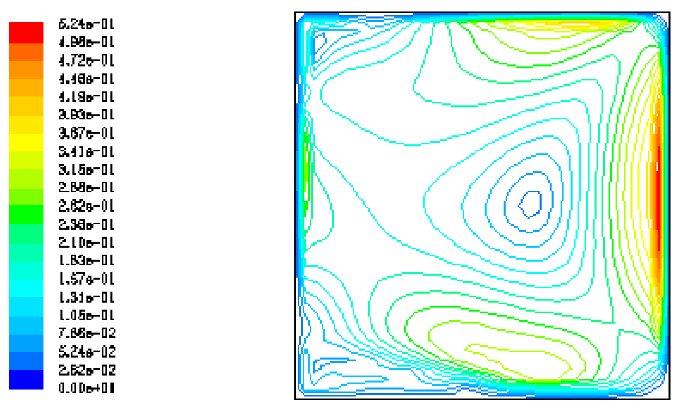

Fig. 6(c). Contours of Velocity Magnitude (m/s) Ra = 1.15×10^{11}.

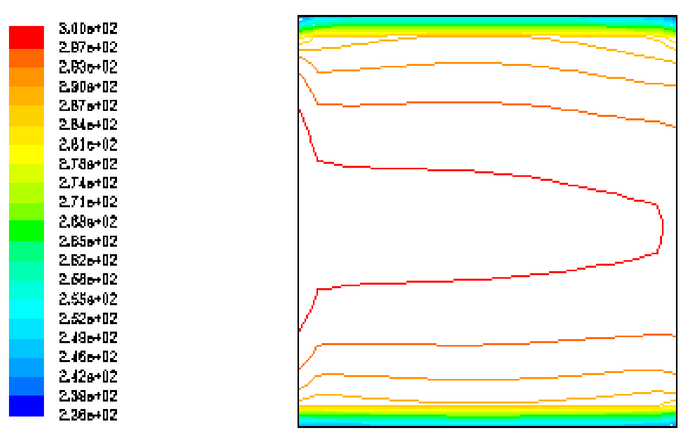

Fig. 7(a). Contours of isotherms (K) Ra = 1.80×10^{9}

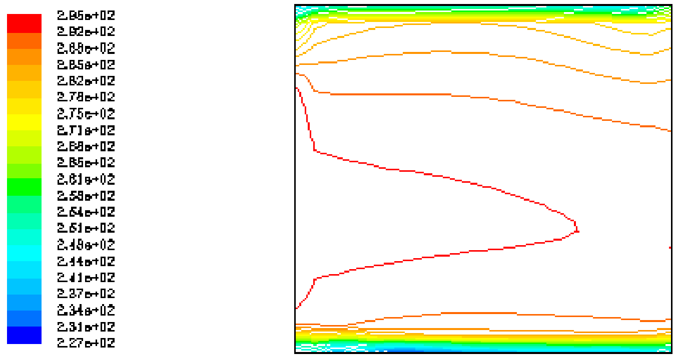

Fig. 7(b). Contours of isotherms (K) Ra = 1.44 × 10^{10}.

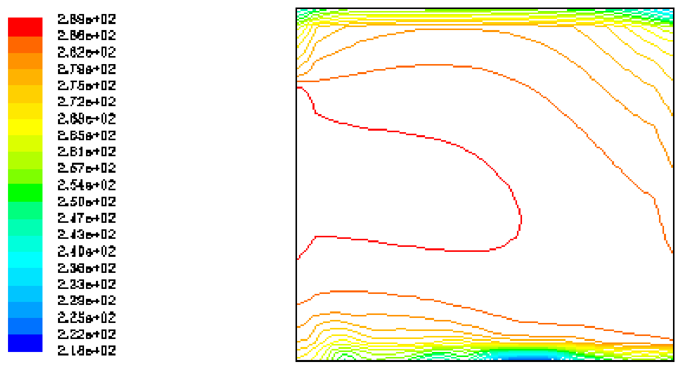

Fig. 7(c). Contours of isotherms (K) Ra = 1.15 × 10^{11}.

5 Conclusion

Numerical simulation of turbulent natural convection in a square enclosure has been done. The study considered an enclosure filled with air with the operating temperature kept at 303K. The temperature difference between the hot wall and the cold wall was kept at 20K, the Rayleigh number varied by varying the length of the enclosure. The modeling of the equations was done to obtain the k and ε equations. The finite volume based solver Fluent with Boussinesq approximation was used on the study. In order to take care of the non – linear character of equations, an iteration procedure was used. The results were presented in terms of the stream functions distribution, contours of velocity magnitudes and isotherms distributions. The results showed that, increasing the length of the enclosure increased the Rayleigh number, the stream functions strengthened consequently increasing the number of vortices. The study enables engineers with reliable results in enhancing electrical, industrial, building and construction engineering applications.

6 Recommendations

In this work a numerical study was performed to predict the solution in natural convection and buoyancy – driven flows in a square enclosure with a fixed aspect ratio. The walls of the enclosure, one was hot and the other opposite wall was relatively cold and the other four walls were totally insulated (adiabatic). From this study it is recommended that further investigations be done in enclosures:-

i. Investigate the enclosure with a case where a heater is introduced at the bottom of the hot wall.
ii. While maintaining the Rayleigh number constant vary the size of the enclosure and investigate the behaviour of streamlines and isotherms distributions.

iii. Introduce a window at the top of the cold wall and analyse the distribution of streamline and isotherms with the results in this study.
iv. Investigate the same enclosure with other models like $k-\omega, SST$ model, RNG $k-\varepsilon$ model because in this case standard $k-\varepsilon$ model was used.

Competing Interests

Authors have declared that no competing interests exist.

References

[1] Batchelor GK. Heat transfer by free convection across a closed cavity between vertical boundaries at different temperature. Applied Mathematics. 1954;12:209–233.

[2] Ozoe HM, Ohmuro M, Churchill SW, Lior N. Numerical calculations of laminar and turbulent natural convection in water and in rectangular channels heated and cooled isothermally on the opposing vertical walls. Int. J. Heat Mass Transfer. 1986;28:125–138.

[3] November M, Nansteel MW. Natural convention in rectangular enclosures heated from below and cooled along one side. Int. J. Heat Mass Transfer. 1987;30:2433-2440.

[4] Lankhorst AM, Hoogendoorn CJ. Numerical computation of high Rayleigh number Natural convection and prediction of hot radiator induced room air motion. Applied scientific Research. 1990; 47(4):301-322.

[5] Gatheri FK, Reizes JA, Leonardi E, Grahamdel VD. Natural convection in an Enclosure with localized Heating and cooling: A numerical study. Heat Transfer. 1990;5:361-3661.

[6] Ganzarolli MM, Milanez LF. Preview of heat and mass transfer. International centre for Heat and mass Transfer. 1995;21:210.

[7] Dol HS, Hanjalic. Computation study of turbulent natural convection in a side heated near-cubic enclosure at a High-Rayleigh number. International Journal of Heat and Mass Transfer. 2001; 44:2323-2344.

[8] Paolucci S, Chenoweath DR. Transition to chaos in differentially heated cavity. J. Fluid Mech. 2006; 2001:379-410.

[9] Geniy VK, Mikhail AS. Numerical Simulation of Turbulent Natural Convection in a Rectangular Enclosure having Finite Thickness Walls. International Journal of Heat and Fluid Flow. 2009;53:163–177.

[10] Formichev AI. Comparison of the results of modelling convective heat transfer in turbulent flows with experimental data. Journal of Engineering Physics and Thermophysics. 2010;83:967–976.

[11] Aksouh M, Amina M, Nassim S, Zaubida H. Raleigh number effect on the turbulent heat transfer within a parallel piped cavity. Journal of Thermal Science. 2011;15:5341-5356.

[12] Betts PL, Bokhari IH. Experiments on turbulent natural convection in an enclosed tall cavity. International Journal of Heat and Fluid Flow. 2000;21(6):675–683.

[13] Eliton F, Adriano DS, Viviana CM. Natural convection in a partially open square cavity with internal heat source: An analysis of the opening mass flow. International Journal of Heat and Mass Transfer. 2011;54:1369–1386.

[14] Shimin W, Zhigang S, Linxia G. Numerical simulation of buoyancy driven turbulent ventilation in attic space under winter conditions. Journal of Energy and Buildings. 2011;47:300-308.

[15] Seok KC, Seong OK. Turbulence modelling of natural convection in enclosures. Journal of Mechanical Science and Technology. 2012;26(1):283–297.

[16] Shati AKA, Blakey SG, Beck SBM. A dimensionless solution to radiation and turbulent natural convection in square and rectangular enclosures. A Journal of Engineering and Technology. 2012; 7(2):257–279.

[17] Sheng C, Hao L, Chuguang Z. Numerical study of turbulent double – diffusive natural convection in a square cavity by LES – based Lattice Boltzmann model. International Journal of Heat and Mass Transfer. 2012;55:4862–4870.

[18] Yuri F, Tim C. Transitional and turbulent naturals convectional in spherical shells. International Journal of Heat and Mass Transfer. 2013;64:514-525.

[19] Claudia Z, Rodion G. Modelling turbulent heat transfer in a natural convection flow. Journal of Applied Mathematics and Physics. 2014;2:662–670.

[20] Yong GP, Manyeong H, Changyoung C, Jaehyun P. Natural convection in a square enclosure with two inner circular cylinders positioned at different vertical locations. International Journal of Heat and Mass Transfer. 2014;77:501-518.

[21] Paulo HSC, Marcelo JS. Turbulent free convection in a porous cavity using the two – temperature model and the High Reynolds closure. International Journal of Heat and Mass Transfer. 2014;79:105–115.

[22] Amano RS, Arakawa H, Suga K. Turbulence heat transfer in a two – pass cooling channel by several wall turbulence models. International Journal of Heat and Mass Transfer. 2014;77:406–418.

[23] Nzomo TK, Awuor KO. A numerical study of turbulent natural convection in a rectangular enclosure using a two – equation turbulence model. Asian Journal of Mathematics and Computer Research. 2017;19:2.

[24] Currie IG. Fundamental of fluids. McGraw – Hill Inc.; 1974.

[25] To WM, Humphrey JAC. Numerical simulation of buoyant, turbulent flow – 1. Free convection along a heated, vertical, flat plates. International Journal of Heat and Mass Transfer. 1986;29:573–592.

[26] Heindel TJ, Ramadhyani S, Incropera FP. Assessment of turbulence models for natural convection in an enclosure. Journal in Numerical Heat Transfer Part B. 2004;26:147–172.

[27] Yap C. Turbulent heat and momentum transfer in recirculating and impinging flows: PhD Thesis, Faculty of Technology, University of Manchester; 1987.